Supporting Information

Vincenz and Kerppola 10.1073/pnas.0805317105

SI Results

Design of Fusion Proteins for BiFC Analysis of CBX Protein Interactions. BiFC analysis is based on formation of a fluorescent complex by complementary fluorescent protein fragments fused to interacting proteins (1). We expressed each CBX protein fused to a fluorescent protein fragment together with histone H3 fused to the complementary fragment. Binding of the CBX fusion to chromatin containing the H3 fusion was predicted to facilitate BiFC complex formation. To minimize the possibility that the fusions had differential effects on individual CBX proteins or BiFC complexes, the fragments as well as intact fluorescent proteins were fused to the N-termini of these proteins, in the same position relative to the conserved chromodomain of each CBX protein. Each H3 variant was fused to the complementary fluorescent protein fragment at its C terminus, a position shown in *Tetrahymena* H3 not to interfere with genetic complementation of H3 mutations (2). We observed similar efficiencies of BiFC complex formation by all CBX proteins with each H3 variant (Fig. S5*F*). We focused on CBX protein interactions with H3.2 in ES cells and MEFs because H3.2 has the highest level of K27-trimethylation (3). We also investigated CBX protein interactions with H3.1 in COS1 cells because H3.1 is the most abundant H3 variant in transformed cells. Fusion of the fluorescent protein fragment to the N terminus of H3.1 produced similar relative efficiencies of BiFC complex formation with CBX protein mutants in COS1 cells (data not shown). However, whereas the C-terminal fusions to all H3 variants were trimethylated on K27, the N-terminal fusion eliminated K27 trimethylation (data not shown). We therefore focused on C-terminal fusions to H3.1 and H3.2.

Levels of Endogenous and Transiently Expressed Exogenous CBX Proteins in ES Cells. We examined the expression of endogenous CBX proteins in ES cells to identify the CBX proteins expressed in ES cells and to compare their levels of expression with those of the CBX fusions. Endogenous CBX6 and CBX7 were expressed at the highest levels in ES cells (Fig. S2). CBX2 was expressed at a lower level, and CBX8 was only detectable after induction of ES cell differentiation (data not shown). None of the available antibodies detected endogenous CBX4 in the cell lines tested. Whereas endogenous CBX2, CBX6, and CBX7 were readily detectable in ES cells by immunoblotting using antibodies specific for each CBX protein, the CBX fusions that were transiently expressed under the conditions used for the imaging experiments were barely detectable by these antibodies. We therefore used a mixture of antibodies specific for the relevant CBX protein and for GFP to compare the levels of expression of different CBX protein fusions (Fig. 2). On the basis of the transfection efficiencies determined by flow cytometry, we estimate that the average levels of CBX6 and CBX7 fusion protein expression in transfected ES cells were lower than those of the corresponding endogenous proteins and that the level of the CBX2 fusion was at most twofold higher than that of endogenous CBX2. Thus, the BiFC assay enabled detection of chromatin association by CBX proteins expressed at levels similar to or lower than those of endogenous CBX proteins. We also examined the properties of CBX2 and CBX6 fusions in stably transfected cells, where the levels of expression were less heterogeneous and could be more accurately quantified (Fig. S7).

Comparison of the Genes Occupied by Endogenous CBX2 and CBX2 Fusions in ES Cells and Cells That Produced CBX2–H3.2 BiFC Complexes. To determine whether the CBX2 fusions in cells containing CBX2–H3.2 BiFC complexes bound to genes that are occupied by endogenous CBX2 in ES cells, we performed ChIP analysis. We used antibodies directed against the FLAG epitope on the CBX2 fusion as well as antibodies against CBX2 to precipitate sheared chromatin from stable ES cell lines that produced CBX2–H3.2 BiFC complexes as well as from the parental ES cell line. Five promoter regions with different H3K4 and H3K27 methylation status were examined: (*i*) Tal1 is only methylated on H3K27, (*ii*) HoxA1 and HoxA11 are well-characterized PcG targets with H3K4 and H3K27 "bivalent domain" methylation, (*iii*) Sox2 is highly expressed in ES cells and methylated on H3K4, (*iv*) Myf5 is not methylated at either H3K4 or H3K27, and (*v*) LineL1 repeats encompass 20% of the mouse genome and are devoid of these methylation marks (4–6).

Endogenous CBX2 was associated with the promoters of genes known to be occupied by PcG proteins (Tal1, HoxA1, HoxA11) in the parental ES cell line (Fig. S3*A*). Near-background signals were detected at the Sox2, Myf5, and LineL1 loci. A similar pattern of total CBX2 occupancy was observed when chromatin from cells containing CBX2–H3.2 BiFC complexes was precipitated with anti-CBX2 antibodies (Fig. S3*B*). BiFC complex formation therefore did not alter the total level of occupancy or selectivity of CBX2 binding in these cells. Precipitation of the CBX2 fusion using anti-FLAG antibodies also demonstrated the highest levels of occupancy at the Tal1, HoxA1, and HoxA11 promoters in cells containing CBX2–H3.2 BiFC complexes (Fig. S3*B*). The signals at the Sox2, Myf5, and LineL1 loci observed in these precipitations were close to the background observed when chromatin from the parental cells lacking CBX fusions was precipitated using anti-FLAG antibodies (Fig. S3*A*). The higher background observed with anti-FLAG Sepharose than with Protein G agarose could be due to the difference in the bead matrices. It should also be noted that the percentage of input that is precipitated varies for different antibodies owing to differences in their avidities and the accessibility of the epitopes in cross-linked chromatin. Thus, the CBX2 fusions in cells containing CBX2–H3.2 BiFC complexes bound to the same genes occupied by endogenous CBX2 in ES cells.

As a control to establish whether selective precipitation of the same promoter regions from cells that expressed CBX2–H3.2 BiFC complexes and those that expressed endogenous CBX2 alone reflected preferential solubilization of these chromatin regions, we precipitated chromatin from the parental cells using anti-H3-acetyl-K27 antibodies. This modification was enriched at the Sox2 and HoxA1 genes, demonstrating that these loci could be precipitated from the same chromatin preparation that was used to analyze CBX2 occupancy (Fig. S3*C*). To establish the incorporation of H3.2 fusions in chromatin, we precipitated chromatin from cells that stably expressed H3.2–Venus using anti-GFP antibodies because H3.2 fused to the fluorescent protein fragment was not efficiently precipitated by any of the antibodies tested. H3.2–Venus was associated with most of the loci tested, with the exception of the HoxA11 and Tal1 promoters (Fig. S3*D*). The low occupancy of CBX2 fusions at some promoters was therefore not caused by preferential incorporation of H3.2 fusions at these loci.

Comparison of BiFC Signals Between Cells That Expressed Different CBX Mutants and Between Wild-Type and EED Null ES Cells. Differences in BiFC complex formation by CBX mutants could be due

to many factors unrelated to protein interactions, including the efficiency of association by the fluorescent protein fragments as well as the levels of expression of the fusion protein. In COS1 cells, the fusion proteins were expressed at comparable levels (Fig. S5 *A–E*). We compared the effects of CBX mutations on BiFC complex formation with H3.1 vs. Ring1B, to distinguish specific effects of mutations on one or the other interaction from potentially general effects of the mutations on fragment association. If a mutation has differential effects on BiFC complex formation with H3.1 and Ring1B, it is likely that the mutation specifically affects one or the other interaction. However, if a mutation has equivalent effects on BiFC complex formation with both partners, it is possible that the mutation affects both interactions or that it alters the efficiency of fluorescent protein fragment association independent of changes in protein interactions.

In ES cells, some of the CBX mutants were expressed at higher levels than the corresponding wild-type proteins, whereas the CBX and H3.2 fusions were expressed at lower levels in cells containing H3.2 lacking the N-terminal tail. The intensity of BiFC signal is linearly related to changes in the level of the fusion protein expressed at limiting concentration (A. Robida and T.K.K., unpublished results). H3.2 fusions were expressed in two- to fourfold molar excess relative to CBX fusions to the same epitopes. We therefore corrected the mean fluorescence intensities of the cells for differences in the levels of CBX fusion protein expression determined by immunoblotting extracts of the cells analyzed flow cytometry.

It is possible that differences between the characteristics of different cell types affect the fluorescence intensities produced by BiFC complexes for reasons unrelated to the efficiencies of protein interactions. To compare the efficiencies of BiFC complex formation in wild-type and EED null ES cells, we determined the normalized fluorescence intensities of cells that expressed H2A and H4 fused to complementary fluorescent protein fragments. There was a less than twofold difference between the normalized fluorescence intensities of wild-type and EED null ES cells that expressed these fusions. The efficiencies of protein interactions can therefore be compared between these cell lines using BiFC analysis.

Development of Stable Cell Lines with Inducible CBX–H3.2 BiFC Complexes. Whereas transient expression enables comparison of BiFC complex formation by many different mutants in different cell types, it produces a heterogeneous cell population and restricts the time during which interactions can be studied. To overcome these limitations we established stable ES cell lines that expressed the CBX fusions under the control of a doxycycline-inducible promoter and the H3.2 fusion constitutively at less than 1% of the level of total cellular H3. We focused on CBX2 and CBX6 because they were expressed in ES cells, had distinct distributions both when free and when associated with chromatin, and were differentially affected by deletion of the chromodomain.

Several lines that expressed different inducible levels of the CBX2 and CBX6 fusions together with the H3.2 fusion were isolated. The morphology and growth of cells that expressed the CBX2 fusion were similar to those of the parental line. Lines that expressed the CBX6 fusion had slower growth rates and formed clusters when grown on gelatin-coated plates. The time-course of BiFC complex formation and disappearance closely followed the induction and depletion of CBX2 fusion protein expression in response to doxycycline addition and withdrawal (Fig. S7). For the imaging and iBiSC experiments, we used induction conditions that produced exogenous CBX protein levels less than fivefold higher than those of the corresponding endogenous proteins.

The distributions of the CBX2–H3.2 and CBX6–H3.2 BiFC complexes in the stable cell lines were similar to those observed in transiently expressing cells (compare Fig. 3 *A* and *B* with Fig. 1 *A* and *C*). CBX2–H3.2 BiFC complexes were more completely localized to chromocenters in the stable cell lines than in transiently expressing cells and were associated with a subset of the chromocenters. The distributions of the BiFC complexes remained stable over several weeks of inducible expression, indicating that the level and duration of fusion protein expression did not affect BiFC complex localization. CBX2–H3.2 BiFC complexes had a distribution distinct from endogenous CBX2, which was distributed in a granular pattern that was excluded from regions resembling nucleoli (Fig. 3*B*). Conversely, both CBX6–H3.2 and endogenous CBX6 were uniformly distributed in the nucleus (Fig. 3 *C* and *D*). The spots in the immunofluorescence image represent background signal that was not competed by incubation of the antibody with antigen (data not shown). The BiFC complexes were associated with chromosomes during mitosis (Fig. 3*E*), consistent with chromatin association, but were distinct from the bulk of endogenous PRC1 proteins (7).

Time-Course of BiFC Complex Formation in Stable Cell Lines with Inducible CBX2 Fusion Expression. To investigate the dynamics of BiFC complex formation and turnover, we compared the time course of CBX2 fusion protein expression and BiFC complex fluorescence after doxycycline addition and withdrawal. No CBX2 fusion expression or BiFC fluorescence was detected in uninduced cells (Fig. S7*A*). Doxycycline addition produced a rapid increase in expression of the CBX2 fusion and a slightly delayed increase in BiFC complex fluorescence (Fig. S7 *A* vs. *B*). The slight delay in the time course of BiFC complex fluorescence relative to the level of CBX2 fusion expression could be due to the time required for fluorophore maturation. The level of CBX2 fusion expression and fluorescence intensity reached a peak 24 h after induction. The induction was not uniform in the cell population: ≈40% of the cells had no detectable fluorescence and did not express the CBX2 fusion according to immunofluorescence analysis. Subsequently, the level of CBX2 fusion expression and the BiFC signal declined to steady-state levels. Time-lapse imaging indicated that the foci formed by CBX2–H3.2 BiFC complexes were stably maintained over at least 1 h (Movie S1). Upon doxycycline withdrawal, the level of the CBX2 fusion and the fluorescence of BiFC complexes decreased to undetectable levels within 48 h (Fig. S7*C*). The foci formed by CBX2–H3.2 BiFC complexes were therefore dynamic structures subject to continuous turnover and assembly.

Effect of CBX2 Fusion Expression on the Recovery of H3.2 Fusions in iBiSC Analysis. We examined the specificity of H3.2 fusion copurification with the CBX2 fusion by performing iBiSC analysis in the presence and absence of doxycycline. The H3.2 fusion was immunopurified only from cells grown in the presence of doxycycline, demonstrating the specificity of H3.2 fusion copurification with the CBX2 fusion (Fig. S8). Aliquots of the input chromatin and the immunopurified fractions were analyzed by immunoblotting using antibodies directed against GFP to detect the total amounts of the H3.2 fusions, and antibodies directed against trimethyl-K27 and dimethyl-K4 were used to detect the levels of these modifications.

To determine the relative levels of histone modifications in the immunopurified fractions compared with input chromatin, we calculated the ratio of the H3.2 bands between the immunopurified fractions and input chromatin on each blot and compared the ratios between blots probed using antibodies directed against specific histone modifications and the blot probed using antibodies directed against GFP (Fig. S8*A*, compare H3.2–YC bands between immunopurified fractions and input chromatin lanes on different blots). The H3.2 fusion that copurified in CBX2–H3.2

BiFC complexes was enriched in K27 trimethylation and K4 dimethylation (Fig. S8*B*). The reasons for the differences in the levels of enrichment of various modifications in different experiments are not known but may reflect changes in modifications induced by CBX protein binding.

Principles and Interpretation of iBiSC Analysis. iBiSC provides a novel approach for the identification of modifications and interactions associated with a specific protein complex. This approach takes advantage of the stabilization of protein interactions caused by association of the fluorescent protein fragments (1). We estimated the purification factor for the CBX–H3.2 BiFC complexes by measuring the increase in the ratio of the H3.2 fusion to endogenous H3 between the input and immunopurified samples (Fig. 4*A*, lanes 4 and 3). This ratio increased 250–400-fold, which represents the minimum purification factor for the CBX–H3.2 BiFC complex. The reason this represents a minimum estimate is that we expect some endogenous H3 to copurify with CBX–H3.2 BiFC complexes. An independent estimate of the maximum amount of contaminating H3.2 fusions in the immunopurified fractions that were not associated with CBX–H3.2 BiFC complexes can be made on the basis of the fact that no detectable H3.2 fusions were precipitated by FLAG antibodies from cells that did not express CBX fusions (Fig. 4*A*, lane 5 and Fig. S8*A*, lane 1). On the basis of the limit of detection, we estimate that this represents less than 1% of the amount that was coprecipitated from cells that produced CBX–H3.2 BiFC complexes. These estimates suggest that contaminating H3.2 fusions did not materially affect determination of the enrichment of histone modifications in CBX–H3.2 BiFC complexes.

Analysis of histone modifications using iBiSC analysis requires antibodies of the highest specificity and sensitivity. The reason is that the H3.2 fusion is expressed at trace levels of less than 1% of total H3 to avoid potential disruption of chromatin structure by the fusion. Likewise, the CBX fusion is expressed at low levels to avoid potential nonspecific binding. Consequently, only a small proportion of the CBX2 fusion is associated with the H3.2 fusion, and *vice versa*. Any recognition of the unmodified histone by the antibody reduces the apparent enrichment of the modification. Thus, weak signals that show no enrichment are uninterpretable because they could reflect either nonspecific cross-reactivity or the lack of enrichment. We have tested 11 different antibodies directed against nine different histone modifications and have found three antibodies that produce reliable results in iBiSC analysis.

Effects of Mutations in H3.1 on BiFC Complex Formation with CBX2. The enrichment of trimethyl-K27, acetyl-K9, and dimethyl-K4 modifications in H3.2 associated with CBX2 raised the question of whether these modifications affected CBX2 recruitment to chromatin. To determine the roles of K4, K9, and K27 modifications of H3.1 in CBX2 binding, we examined BiFC complex formation by CBX2 with H3.2 mutants in which these residues were substituted by alanines. Cells that expressed H3.1 fusions containing either a K4A or a K9A substitution had 20% lower fluorescence intensities than cells that expressed the wild-type H3.1 fusion (Fig. S9). In contrast, cells that expressed H3.1 containing the K27A substitution had fluorescence intensities that were not significantly different from those in cells that expressed wild-type H3.1. These results suggest a greater role of K4 and K9 modifications than of K27 in CBX2 binding, although the possibilities that these mutations affect nucleosome assembly or that endogenous histones affect these results cannot be excluded.

SI Materials and Methods

Plasmids. CMV-driven expression constructs were used for transient transfection experiments. Full-length YFP or the N-terminal 172 aa of Venus (VN) were fused to the N-termini of human CBX proteins as described previously (8). Full-length Venus or amino acids 173–238 of YFP (YC) were fused to the C-termini of H3.1, H3.2, and H3.3 (8). The CBX mutations were as follows: (*i*) loss of function mutation analogous to *Drosophila melanogaster* Pc I31F, CBX2 I17F, CBX-4, 6, 7, 8 I16F; (*ii*) ΔChr, deleted amino acids: CBX2 (1–66), CBX4 (1–75), CBX6 (1–95), CBX7 (1–95), CBX8 (1–76); (*iii*) ΔBox, deleted amino acids: CBX2 (499–533), CBX4 (531–556), CBX6 (367–413), CBX7 (220–252), CBX8 (358–390); (*iv*) ΔChr, ΔBox: combination of deletions of (*ii*) and (*iii*). Tailless H3.1, H3.2, and H3.3 lack the 34 N-terminal residues (9). To generate stable ES cell lines, H3.2–YC was subcloned into pKJ1ΔF containing the phosphoglycerate kinase (PGK) promoter and polyA sequence (10) and cotransfected with PGKneo (PGK-driven neomycin resistance). VN-CBX sequences were subcloned into pTRE tight (Clontech) for doxycycline regulatable expression. The doxycycline transactivator (rtTA2^S-M2) (11) was expressed from a strong synthetic ES cell promoter, CAGGS (12), in a plasmid that also expressed Hygromycin resistance from the PGK promoter.

Cell Lines. PGK12.1, a wild-type murine ES cell line, was provided by Neil Brockdorff (13) and cultured on gelatin-coated substrate in DMEM supplemented with 20% FBS, L-Glu, Pen/Strep, nonessential amino acids, 0.1 mM β-S-EtOH, and LIF (10^3U/ml). EED null ES cells were provided by Terry Magnuson and cultured on irradiated MEFs in MEM-α with the same supplements as for PGK12.1 except for nonessential amino acids (14). MEFs were isolated from day-16 embryos and obtained from the University of Michigan transgenic core and used for transient expression experiments or irradiated for use as feeders during ES cell culture.

Transfections. COS1 cells were cotransfected in six-well plates with 0.4 μg VN-CBX, 0.4 μg YC-H3.1, and 0.2 μg CFP using 3 μl of FuGene according to the manufacturer's protocol (Roche). MEF cells (2×10^6) were transfected with 9 μg of VN-CBX and 4.5 μg of H3.2–YC using MEF 1 nucleofector kit (pulse A23) (amaxa). The mouse ES nucleofector kit (pulse A23) was used for ES and EED null cells (4×10^6) with 9 μg VN-CBX, 4.5 μg H3.2–YC, and 2 μg CFP. Cells were plated on a gelatin-coated 10-cm dish and analyzed 24 h later. For stable transfection of ES cells, plasmids were linearized and electroporated with BioRad Gene Pulser II (250 μF, 0.3 Kev). For 8×10^6 cells 2 μg of the plasmid carrying the selection marker and 18 μg of the plasmid lacking the marker were used. Selection was started 48 h after transfection (0.4 mg/ml G418 or 0.2 mg/ml Hygromycin). Selection was removed once the clones were transferred to 24-well plates. Positive clones were identified by Western blotting.

Fluorescence Microscopy. BiFC complexes and total populations of CBX proteins in transiently expressing cells were imaged 24 h after transfection. For live cell imaging, cells were grown on coverslips, stained with 10 ng/ml Hoechst for 10 min, washed with PBS, and visualized in DMEM without phenol red at 37°C. Live ES and MEF cells were visualized by conventional fluorescence microscopy using an Olympus IX70 microscope equipped with a ×100 oil objective and a CoolSNAP HQ2 monochrome camera. Confocal images of stable lines were obtained using a ×100 oil objective on an Olympus IX81 microscope equipped with a Disk Spinning Unit and a Hamamatsu ORCA-ER camera. For fixed cells, an Olympus BX60 microscope equipped with a ×100 oil objective and an Olympus DP70 color camera was used.

Flow Cytometry. Thirty-six hours after transfection COS1 cells were incubated for 2 h at 30°C, harvested in citrate solution (0.135 M NaCl, 15 mM NaCitrate, 15 min at 37°C), washed in PBS, fixed with 1% formaldehyde for 1 h at 4°C, washed in PBS, and analyzed on a BD Biosciences FACSAria High-Speed Flow Sorter. The BiFC and CFP signals were quantified using 488-nm and 407-nm excitation. Gates for BiFC- and CFP-positive cells were set to exclude 99.5% of nontransfected cells. The mean fluorescence intensities of the BiFC complexes were normalized by the mean fluorescence intensity of coexpressed CFP (Normalized fluorescence = BiFC fluorescence/CFP fluorescence). ES and EED null ES cells were incubated 20 h at 37°C and 4 h at 30°C after transfection, harvested in citrate solution, washed in PBS, and analyzed by flow cytometry without fixation. For ES and EED null ES cells, the normalized fluorescence intensities were adjusted to account for differences in the expression levels of the CBX mutants relative to the wild-type protein, as measured by Western blot analysis (Corrected fluorescence = Normalized fluorescence/Relative expression level). In each experiment, 15,000 transfected COS1 cells or 20,000 transfected ES cells were analyzed. Cell lysates were prepared from the same population of cells and analyzed by Western blotting.

Immunocytochemistry. Cells were grown on gelatin-coated coverslips, fixed with fresh 4% formaldehyde in DMEM for 10 min at 4°C, washed twice with PBS, and permeabilized with 0.2% Triton X-100 at room temperature for 10 min. The coverslips were blocked with 3% BSA, 3% normal goat serum in PBS for 1 h at room temperature, followed by incubation with primary antibody overnight at 4°C. Primary and secondary antibodies were diluted in 3% BSA, 3% normal goat serum, and 0.1% Tween 20. After three washes with PBS, the samples were incubated with secondary antibody for 1 h at room temperature. Three final washes with PBS were done, Hoechst 10 μg/ml was included in the second wash when required, and the samples were mounted with ProLong Gold (Invitrogen). The antibodies and conditions used are listed in Table S2.

Metaphase Spreads. Metaphase spreads were prepared according to classic protocols (15) but without methanol acetic acid fixation to preserve BiFC complex fluorescence. The inducible CBX2 and CBX6 ES cell lines were grown to approximately 50% confluence before adding doxycycline (1 μg/ml). After 4 h the culture was transferred to 30°C for 16 h, followed by a 2-h incubation at 37°C and addition of demecolcine (50 ng/ml) for 1 h. The media were harvested and pooled with the cells harvested by trypsinization. Cells (1×10^6) were washed in 5 ml PBS. The cell pellet was resuspended in a 50-ml tube with 200 μl of PBS, 1 ml of 75 mM KCl was added dropwise with constant gentle agitation, and the cells were incubated at room temperature for 5 min. An additional 7 ml of 75 mM KCl was added, followed by gentle rocking of the tube. The cells were swollen for another 10 min before loading 60–120 μl into cytofunnels (Shandon). Cells were cytospun for 5 min at 2,000 rpm onto a glass slide (Shandon cytospin3), washed in PBS, fixed, and Hoechst stained in 4% paraformaldehyde and 10 μg/ml Hoechst, washed again, and mounted using ProLong Gold.

Chromatin Immunoprecipitation. Chromatin immunoprecipitations were performed as described previously (16) with the following modifications. Fixation was with 1.37% paraformaldehyde for 15 min at room temperature. Sonication was performed in 1.5-ml TPX tubes loaded with 300 μl of fixed and extracted nuclei using 60 × 30-sec bursts at full power in a Bioruptor XL (Diagenode) sonicator, yielding soluble chromatin (0.2–1 kb). Immunocomplexes were harvested using Protein G beads and washed five times with RIPA buffer (50 mM Hepes-KOH, 500 mM LiCl, 1 mM EDTA, 1% Nonidet P-40, and 0.7% Na-deoxycholate) and twice with TE (50 mM NaCl, 1 mM EDTA, and 10 mM Tris [pH 8.0]) before reversing the cross-links at 65°C overnight. Quantitative PCR was performed with SYBR green reagents from TaKaRa on an Eppendorf Mastercycler ep realplex with the primers listed in Table S3.

Isolation of BiFC Stabilized Complexes. iBiSC was performed under the same conditions as ChIP analysis but without cross-linking (16). Five 15-cm plates were grown to 80% confluence and doxycycline was added, followed by transfer to 30°C 5 h later. After 20 h of induction, the cells were harvested, lysed, and the nuclear material washed as for ChiP experiments. Chromatin was solubilized in two steps. First, a homogenous suspension was obtained by sonication with a Branson Sonifier cell disruptor 200 (seven bursts of 20 sec with microtip, output 5, duty cycle 60%), then 300 μl aliquots were sonicated using a BioRuptor for 20 × 30-sec bursts at full power, yielding soluble chromatin (200–500 bp). Triton X-100 was added to 1% and insoluble material removed by 20,000 × g centrifugation for 10 min. The soluble chromatin was precleared with 200 μl protein G for 2 h and represents the input material. FLAG beads (60 μl of 50% suspension) were added and incubated overnight. The FLAG beads were washed as follows: 3 × 1 ml wash with low-salt buffer (20 mM Tri-HCl [pH 8.1], 150 mM NaCl, 1 mM EDTA, 0.1% SDS, and 1% Triton X-100), 2 × 1 ml high-salt buffer (20 mM Tri-HCl [pH 8.1], 500 mM NaCl, 1 mM EDTA, 0.1% SDS, and 1% Triton X-100), 3 × 1 ml TE. The beads were boiled in 150 μl SDS-PAGE loading buffer, and soluble proteins were separated on 4%–12% NuPage BisTris gel.

To determine the enrichment of histone modifications in the iBiSC experiments, a series of exposures was obtained for each Western blot in such a way that several bands were in the linear range of the film from different exposures. This allowed the calculation of conversion factors between different exposures. The optical densities of bands were quantified using ImageJ 1.37v. The ratio between the signals for immunoprecipitated and input material was compared between blots probed with a modification-specific (i.e., anti-H3 acetyl-K9) antibody and antibodies recognizing total protein (i.e., anti-GFP and anti-H3).

1. Hu CD, Chinenov Y, Kerppola TK (2002) Visualization of interactions among bZIP and Rel family proteins in living cells using bimolecular fluorescence complementation. *Mol Cell* 9:789–798.
2. Cui B, Liu Y, Gorovsky MA (2006) Deposition and function of histone H3 variants in Tetrahymena thermophila. *Mol Cell Biol* 26:7719–7730.
3. Hake SB, *et al.* (2006) Expression patterns and post-translational modifications associated with mammalian histone H3 variants. *J Biol Chem* 281:559–568.
4. Boyer LA, *et al.* (2006) Polycomb complexes repress developmental regulators in murine embryonic stem cells. *Nature* 441:349–353.
5. Azuara V, *et al.* (2006) Chromatin signatures of pluripotent cell lines. *Nat Cell Biol* 8:532–538.
6. Martens JH, *et al.* (2005) The profile of repeat-associated histone lysine methylation states in the mouse epigenome. *EMBO J* 24:800–812.
7. Buchenau P, Hodgson J, Strutt H, Arndt-Jovin DJ (1998) The distribution of polycomb-group proteins during cell division and development in *Drosophila* embryos: Impact on models for silencing. *J Cell Biol* 141:469–481.
8. Ren X, Vincenz C, Kerppola TK (2008) Changes in the distributions and dynamics of polycomb repressive complexes during embryonic stem cell differentiation. *Mol Cell Biol* 28:2884–2895.
9. Ahmad K, Henikoff S (2002) The histone variant H3.3 marks active chromatin by replication-independent nucleosome assembly. *Mol Cell* 9:1191–1200.
10. McBurney MW, *et al.* (1991) The mouse Pgk-1 gene promoter contains an upstream activator sequence. *Nucleic Acids Res* 19:5755–5761.
11. Urlinger S, *et al.* (2000) Exploring the sequence space for tetracycline-dependent transcriptional activators: Novel mutations yield expanded range and sensitivity. *Proc Natl Acad Sci USA* 97:7963–7968.

12. Niwa H, Yamamura K, Miyazaki J (1991) Efficient selection for high-expression transfectants with a novel eukaryotic vector. *Gene* 108:193–199.
13. Penny GD, Kay GF, Sheardown SA, Rastan S, Brockdorff N (1996) Requirement for Xist in X chromosome inactivation. *Nature* 379:131–137.
14. Morin-Kensicki EM, Faust C, LaMantia C, Magnuson T (2001) Cell and tissue requirements for the gene eed during mouse gastrulation and organogenesis. *Genesis* 31:142–146.
15. Tjio JH, Levan A (1956) The chromosome number of man. *Hereditas* 42:1–6.
16. Lee TI, *et al.* (2006) Control of developmental regulators by Polycomb in human embryonic stem cells. *Cell* 125:301–313.
17. Stock JK, *et al.* (2007) Ring1-mediated ubiquitination of H2A restrains poised RNA polymerase II at bivalent genes in mouse ES cells. *Nat Cell Biol* 9:1428–1435.
18. Ishizuka T, Lazar MA (2003) The N-CoR/histone deacetylase 3 complex is required for repression by thyroid hormone receptor. *Mol Cell Biol* 23:5122–5131.

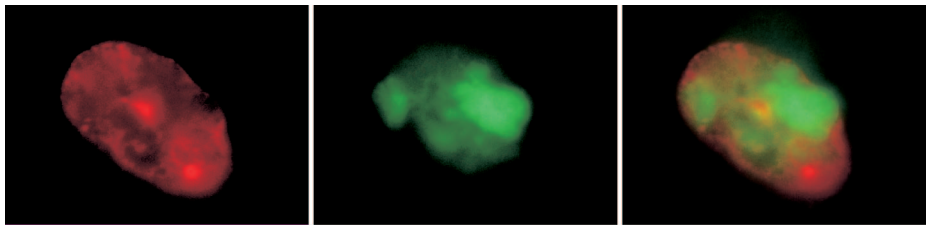

Fig. S1. Distributions of BiFC complexes formed with tailless histone H3.2. Images of the BiFC (green), Hoechst (red) fluorescence, and the merged images are shown for a MEF cell that expressed CBX4 and tailless histone H3.2. Note that the number of cells with detectable fluorescence and the mean fluorescence intensity were much lower, as shown by the flow cytometry quantitation in Fig. 2.

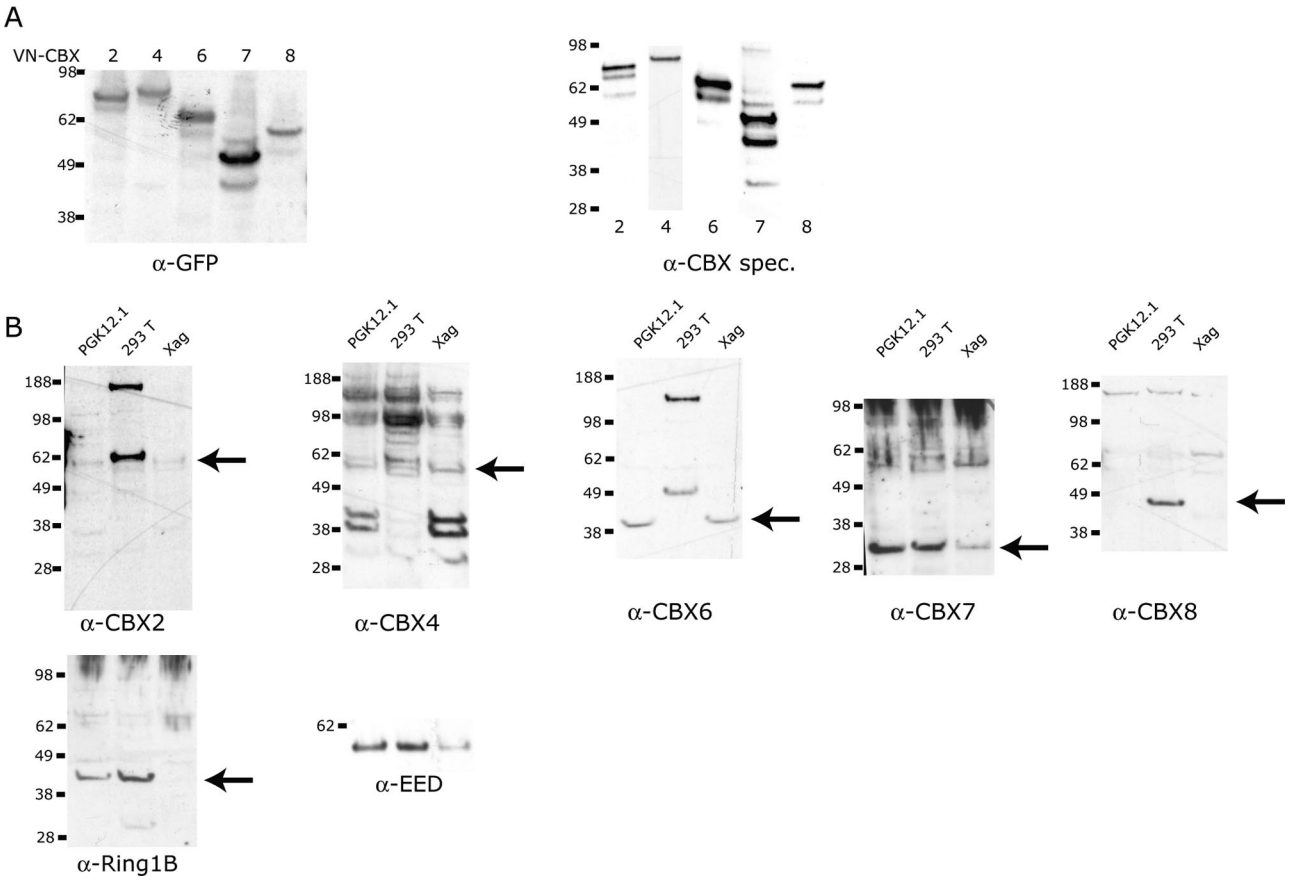

Fig. S2. Characterization of antibodies specific for individual CBX proteins and comparison of CBX protein expression levels. (*A*) Sensitivities of antibodies directed against different CBX family proteins. Transiently expressed CBX fusions were analyzed by immunoblotting using anti-GFP antibodies to determine the relative amounts of different CBX fusions in the extracts. The same lysates were analyzed by CBX-specific antibodies on parallel gels loaded with 1/40 of the amount used for the anti-GFP blot. All exposures were 5 sec except for the anti-CBX4 blot, which was exposed 3 min. (*B*) Levels of endogenous CBX proteins. Whole-cell lysates were analyzed from the mouse ES cell line PGK12.1, human kidney epithelial line 293T, and mouse plasmacytoma line Xag. The exposures shown are 3 min except for CBX4, which were 1 h. The predicted mobilities of the endogenous proteins are indicated by arrows.

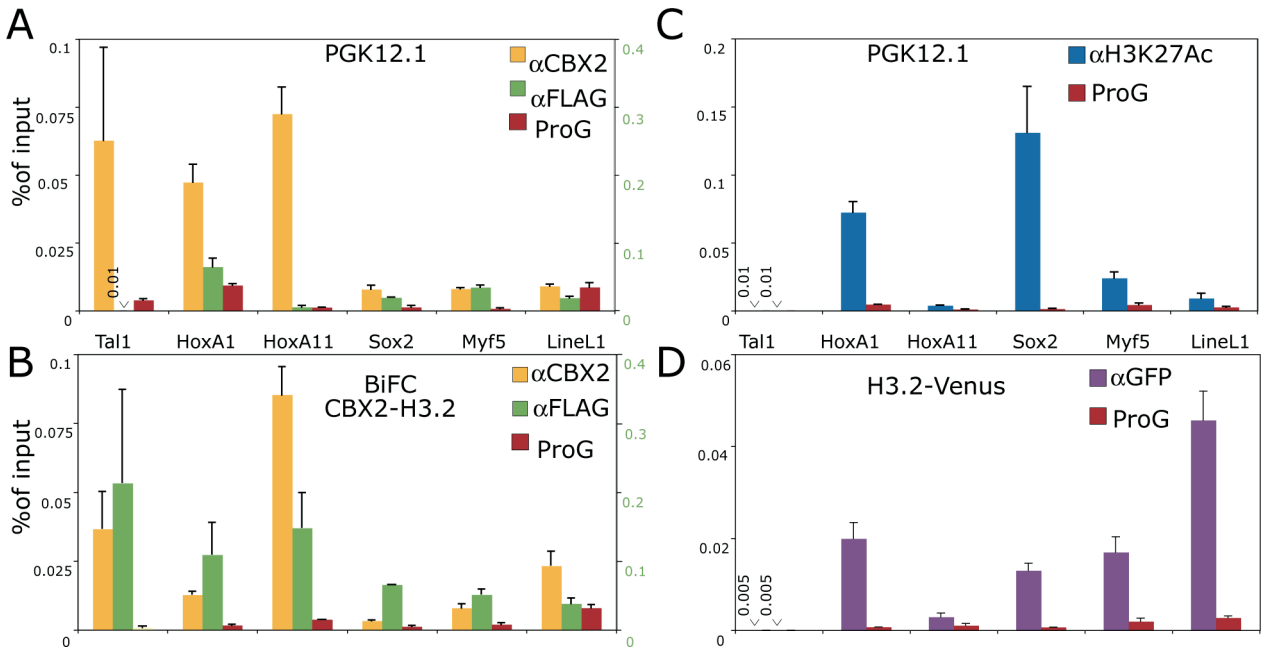

Fig. S3. Comparison of promoter occupancy by endogenous CBX2 and FLAG-tagged CBX2 fused to a fluorescent protein fragment in the parental and CBX2–H3.2 BiFC ES cells. (*A*) ChIP analysis of endogenous CBX2 occupancy in the parental ES cell line. Chromatin from PGK12.1 ES cells was precipitated using CBX2 antibodies (orange) as well as anti-FLAG Sepharose (green) and Protein G agarose (red) as controls. The precipitates were analyzed by quantitative PCR using primer pairs specific for the loci indicated below the bars and compared with the input chromatin. The scale for FLAG ChIP is shown on the right side (green). (*B*) ChIP analysis of total CBX2 (orange) and FLAG-tagged CBX2 fusion (green) occupancy in cells that produced CBX2–H3.2 BiFC complexes at the loci indicated above the bars. (*C*) ChIP analysis of H3 K27 acetylation (dark blue) at the loci indicated below the bars in parental ES cells. (*D*) ChIP analysis of H3.2–Venus occupancy (violet) at the loci indicated above the bars detected by anti-GFP antibody precipitation from cells that stably expressed this fusion.

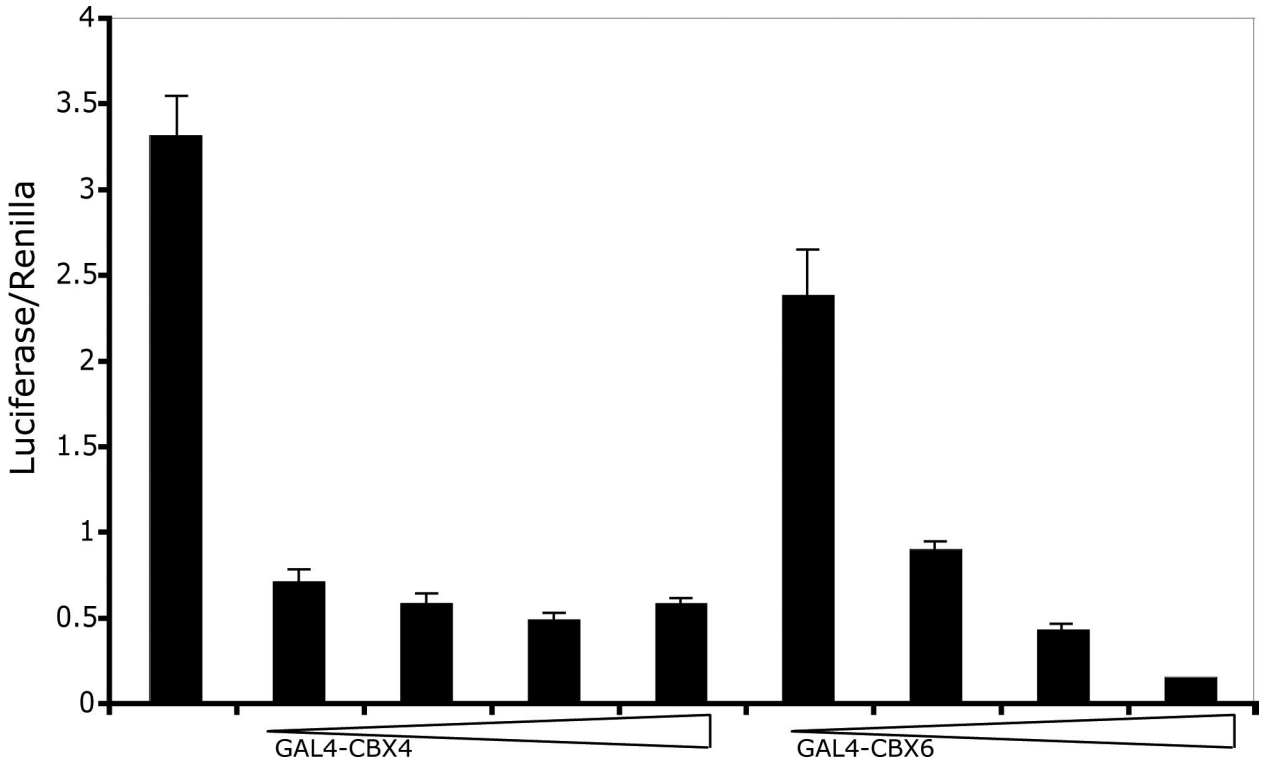

Fig. S4. Transcription repression by CBX4 and CBX6 fused to the GAL4 DNA binding domain at their N-termini. (*A* and *B*) Different amounts (50, 100, 200, 500 ng) of plasmids encoding the GAL4–CBX4 and GAL4–CBX6 fusions were transfected into HEK293T cells carrying an integrated luciferase reporter gene controlled by a synthetic promoter containing 5 GAL4 binding sites (18). The luciferase activities were measured in cell extracts prepared 24 h after transfection and were normalized by the *Renilla* luciferase activity.

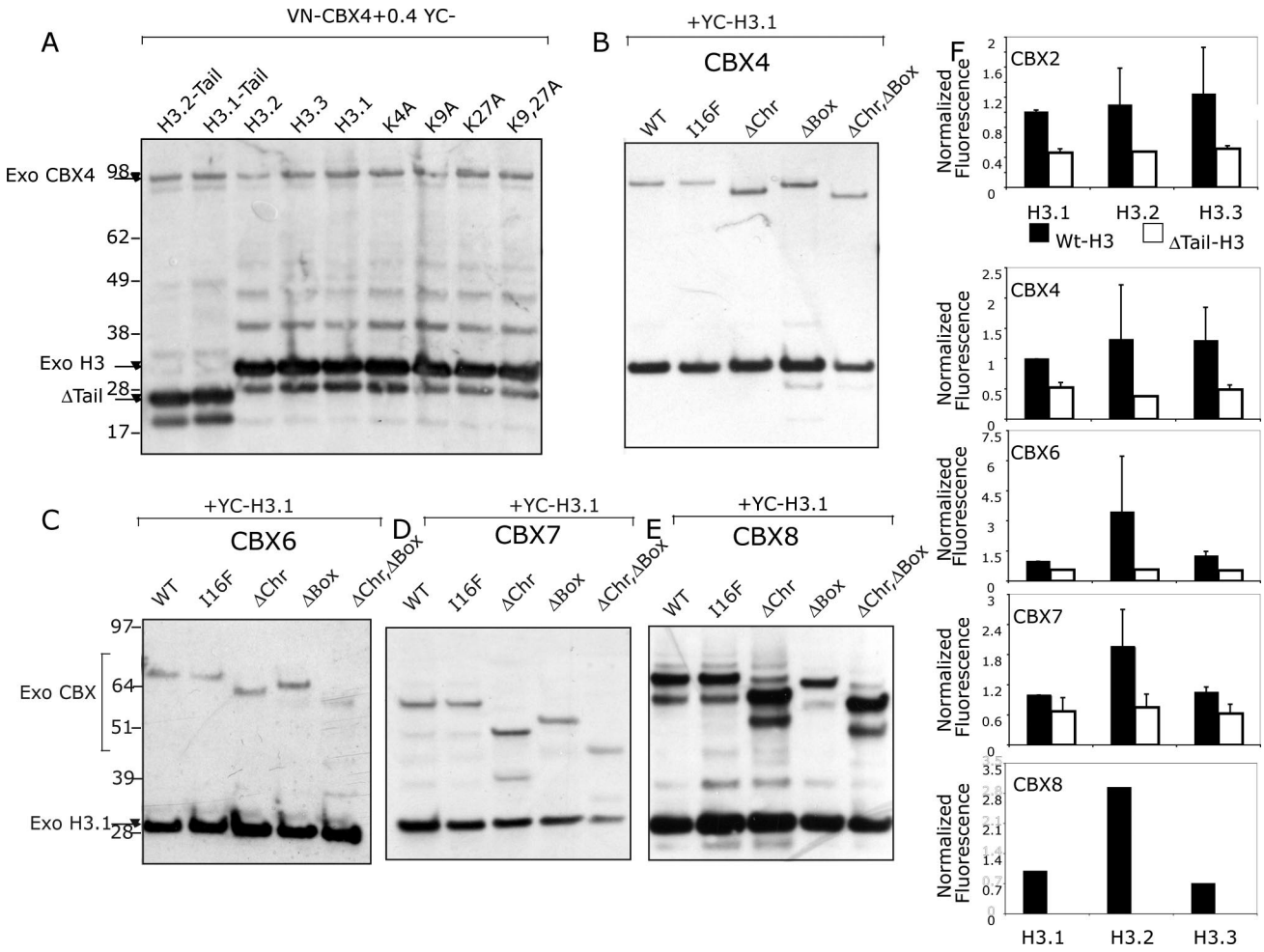

Fig. S5. Expression levels of CBX fusion proteins and BiFC analysis of CBX protein interactions with H3 variants in COS1 cells. (*A*) Plasmids encoding H3 deletions, sequence variants, and point mutants as well as CBX4 fused to complementary fluorescent protein fragments were cotransfected into COS1 cells as indicated and the resulting cell lysates analyzed by anti-GFP Western blot. Plasmids encoding wild-type and mutant CBX4 (*B*), CBX6 (*C*), CBX7 (*D*), and CBX8 (*E*) proteins were similarly coexpressed with H3.1 and analyzed by Western blotting. (*F*) One BiFC fusion of the three sequence variants of H3 or their tailless counterparts were cotransfected with complementary fusions of the different CBX proteins in COS1 cells, and fluorescence was measured using flow cytometry as described for Fig. 2.

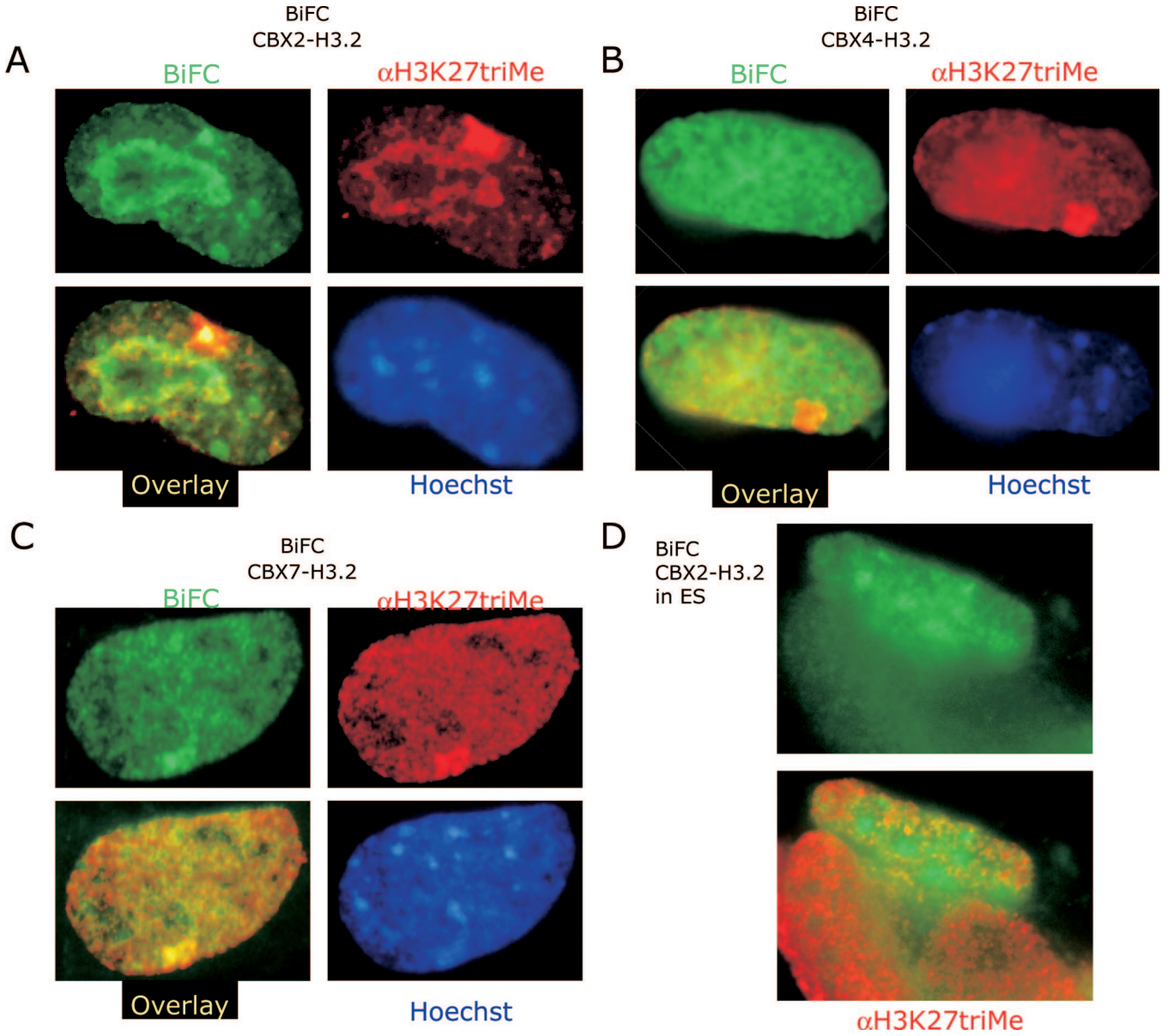

Fig. S6. Comparison of the distributions of CBX-H3 BiFC and anti-H3-trimethyl-K27 immunofluorescence. (*A*) MEF cells were cotransfected with plasmids encoding CBX2 and H3.2 fusions and immunostained using anti-H3-trimethyl-K27 antibodies (red) after 24 h. The bright red spot corresponds to the inactive X that is also enriched in CBX2–H3.2 BiFC complexes. The ring-like accumulation was observed in a large proportion of MEF cells that produced CBX2–H3.2 BiFC complexes and correlated with high fluorescence intensity. (*B*) Same as in *A*, but for CBX4–H3.2 BiFC complexes. (*C*) Same as in *A*, but for CBX7–H3.2 BiFC complexes. (*D*) An ES cell line that stably produced CBX2–H3.2 BiFC complexes (described in Fig. 3) was induced with doxycycline overnight and immunostained using anti-H3-trimethyl-K27 antibodies (red).

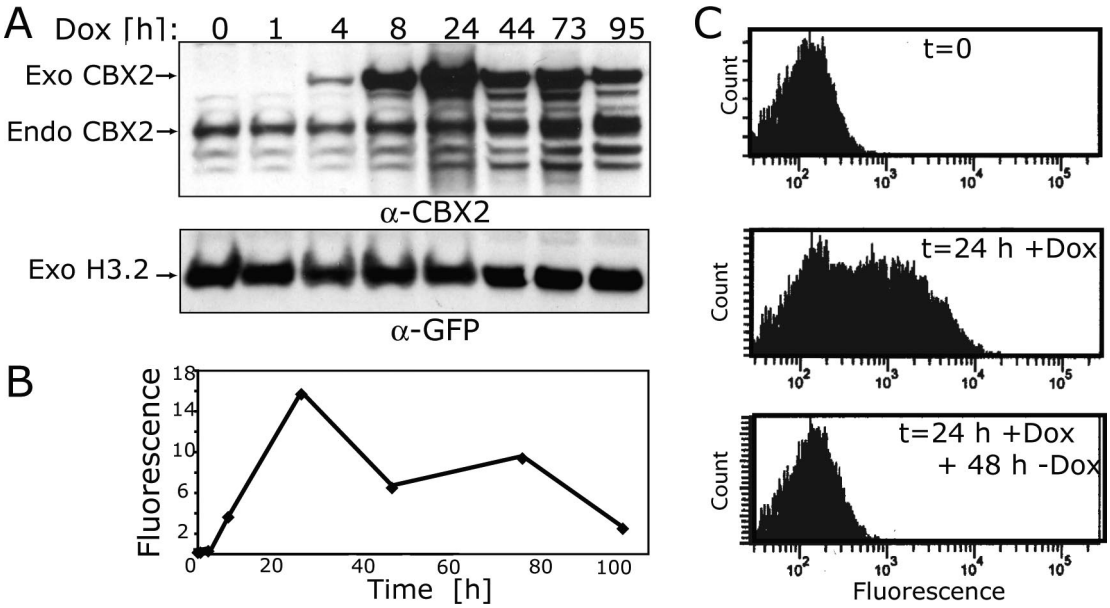

Fig. S7. Comparison of the time courses of CBX2 fusion protein expression and CBX2–H3.2 BiFC complex formation. (*A* and *B*) Time course of CBX2 fusion protein expression and CBX2–H3.2 BiFC complex formation, respectively, after addition of doxycycline. Cells that were stably transfected by inducible CBX2 and constitutive H3.2 fusion constructs (described in Fig. 3) were harvested at the times indicated after induction with doxycycline. Part of the cells were lysed and analyzed by immunoblotting using anti-CBX2 (*Upper*) and anti-GFP (*Lower*) antibodies. The remaining cells were analyzed by flow cytometry, and their mean fluorescence intensities were plotted as a function of the time after doxycycline addition. (*C*) Dynamics of CBX2–H3.2 BiFC complex formation and disappearance after doxycycline addition and removal. The fluorescence intensities of cells described in *A* and *B* were measured by flow cytometry before treatment (*Top*), 24 h after doxycycline addition (*Middle*), and 48 h after doxycycline removal (*Bottom*).

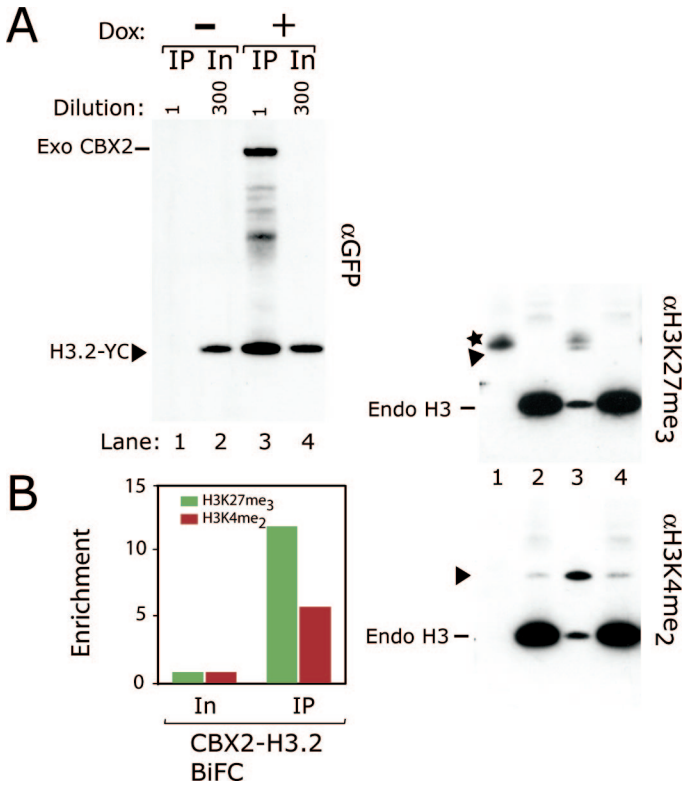

Fig. S8. Effects of CBX2 fusion expression on the recovery of H3.2 fusions in iBiSC analysis. (*A*) Chromatin was isolated from the stable cell lines that contained expression vectors encoding the CBX2 and H3.2 fusion proteins grown in the presence or absence of doxycycline, as indicated above the lanes. The chromatin was immunopurified using anti-FLAG (lanes 1, 3) antibodies. The total amounts of H3.2 fusions (αGFP) and H3.2 fusions containing the modifications indicated to the right of each blot were compared in the input (In) and immunopurified (IP) chromatin by immunoblotting analysis. The mobilities of the H3.2–YC bands that were used for quantitation are indicated by solid triangles. The solid star marks a cross-reactive band. (*B*) Enrichment of H3.2 modifications in CBX2–H3.2 complexes. The enrichment of the modifications was calculated as described in materials and methods.

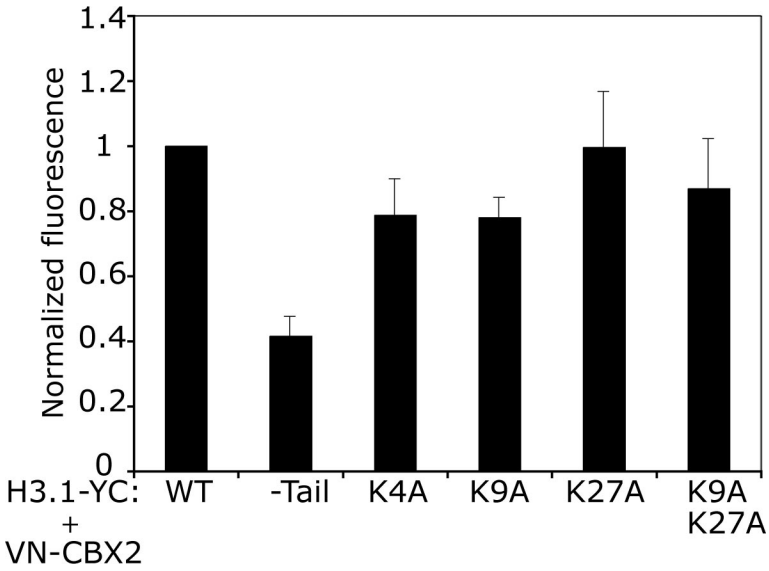

Fig. S9. Effects of single amino acid substitutions in H3.1 on BiFC complex formation with CBX2. The normalized fluorescence intensities of COS1 cells that expressed CBX2 and the indicated H3.1 mutants fused to complementary fluorescent protein fragments were measured by flow cytometry as described in Fig. 2. The data shown represent the mean and SD from at least three independent experiments.

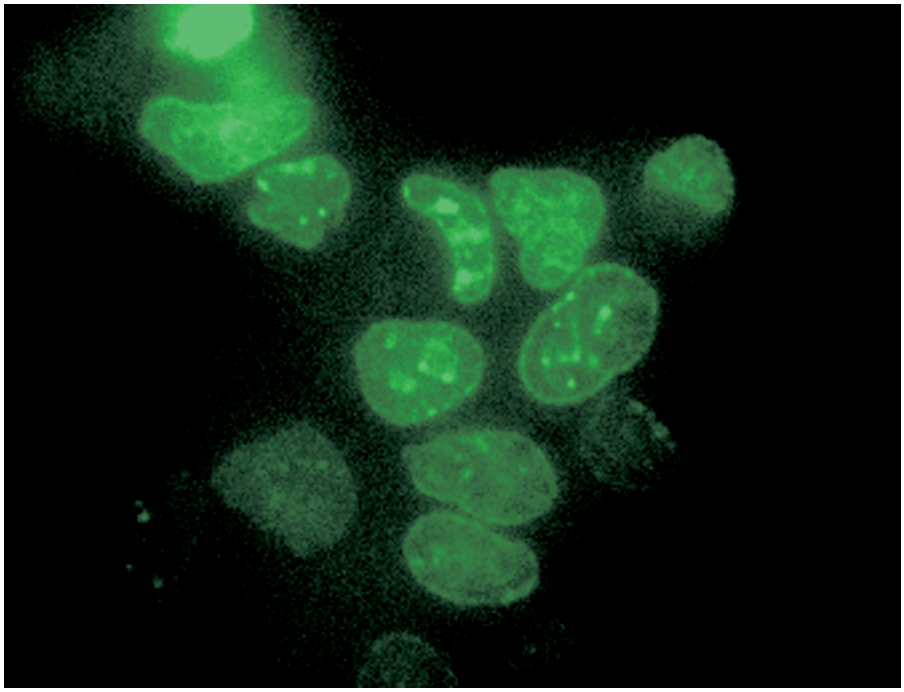

Movie S1. The CBX2 stable cell line (Fig. 3) was treated with doxycycline for 18 h and incubated at 30°C for 2 h before microscopy. A frame was captured every 30 s for 1 h with 4 × 4 pixel binning.

Movie S1 (MOV)

Table S1. Summary of the distributions of YFP–CBX and CBX–H3.2 BiFC complexes

Cell type	Signal	CBX2	CBX4	CBX6	CBX7	CBX8
ES	BiFC	Significant chromocenter localization superimposed on uniform signal	Chromocenter localization. In <30% of cells BiFC signal excluded from regions encompassing chromocenters	Weak and uniform signal	Strong chromocenter localization	Numerous small foci and uniform signal. Weak chromocenter localization
ES	YFP	Numerous foci of different sizes	Many small foci of uniform size	Uniform signal.	Uniform signal with weak chromocenter localization	Uniform signal.
MEF	BiFC	Significant chromocenters localization. Artefactual accumulation of signal that excludes Hoechst stain, particularly in bright cells	Excluded from chromocenters. In <30% of cells accumulation around chromocenters	Weak and uniform signal	Punctate/reticular pattern with excluded regions that contain most chromocenters	Numerous foci of different sizes and uniform signal with excluded regions
MEF	YFP	Numerous foci of different sizes. No uniform signal	Many small foci. No uniform signal	Uniform signal with occasional depletion of signal in chromocenters	Uniform signal with excluded regions that contain most chromocenters	Uniform signal with excluded regions that contain most chromocenters. Punctate signal in bright cells. Weak cytoplasmic signal

The details of the distributions of the BiFC complexes and YFP fusions varied among individual cells in the population. This variation was caused in part by differences in the expression levels of the fusion proteins in individual cells. Overexpression caused accumulation of some of the complexes in regions that excluded Hoechst (i.e., Fig. 1*K*). Nevertheless, the distributions of BiFC complexes formed by all CBX proteins were consistently distinct from those of the corresponding YFP fusions, suggesting that only a subpopulation of each protein was bound to H3.

Table S2. Primary antibodies used in this study

Name	Antigen	Species purification	Dilution for W.B.	Dilution for I.P.	Dilution for I.F.	Dilution for ChIP	Supplier
αCBX2	Peptide P159-T176	Rabbit, Immunogen affinity purified	1:5,000		1:200	1:200	This article
αCBX4	Peptide	Rabbit protein G purified	1:200				Abgent: AP2514b
αCBX6	GST-fusion Y268-S363	Rabbit serum	1:2,000		1:30	1:166	This article
αCBX7	GST-fusion D181-S363	Rabbit serum	1:4,000				This article
αCBX8	GST-fusion E177-D345	Rabbit serum	1:1,000				This article
αRing1B	GST-fusion D172-G307	Rabbit serum	1:1,000				This article
αEED	Peptide C255-R273	Rabbit serum	1:1,000				This article
αGFP	Recombinant full-length GFP	Rabbit protein A purified	1:2,000	1:200	1:100	1:166	RDI: GRNFP4abr
αPanH3	Peptide C-term of H3	Rabbit, Immunogen affinity purified	1:1,000				Abcam: ab1791
αH3K4diMe	Peptide K4diMe	Rabbit, Immunogen affinity purified	1:3,000		1:200		Abcam: ab7766
αH3K9triMe	Peptide K9triMe	Rabbit protein A purified	1:1,000		1:500		Millipore: 07–442
αH3K9Ac	Peptide K9Ac	Rabbit serum	1:5,000				Millipore: 07–352
αH3K27triMe	Peptide K27triMe	Rabbit protein A purified	1:500		1:150		Millipore: 07–449
αH3K27Ac	Peptide K27Ac	Rabbit serum	1:5,000			1:250	Millipore: 07–360
FLAG-M2-beads	Peptide	Mouse agarose beads			12 μl 50% suspension/ml	30 μl 50% suspension/ml	Sigma: A2220

Table S3. Primers used for quantitative PCR

Gene	Primer sequence 5′-3′	Annealing temperature, °C	Ref.
Tal1	F: ttccatcccgttctctcca R: agtccaacaacaacagcctctc	57.7	This article
HoxA1	F: CGA CCA CGC AGA GAT TTT CG R: ACC CAG CCC AGA AAG CTG AA	62.1	(5)
HoxA11	F: AGGAGAAGGGGTTCCTTCAA R: CTCCGCGGTTTGTCAATAAT	60.9	(4)
SOX2	F: CCATCCACCCTTATGTATCCAAG R: CGAAGGAAGTGGGTAAACGCAC	59.7	(5)
MYF5	F: GGAGATCCGTGCGTTAAGAATCC R: GGTAGCAAGACATTAAAGTTCCGTA	55	(17)
LINE L1	F: TTTGGGACACAATGAAAGCA R: CTGCCGTCTACTCCTCTTGG	52.5	(6)

F, forward; R, reverse.